Journal of Molecular Liquids 218 (2016) 39–49

Contents lists available at ScienceDirect

Journal of Molecular Liquids

journal homepage: www.elsevier.com/locate/molliq

Choline salicylate ionic liquid by X-ray scattering, vibrational spectroscopy and molecular dynamics

Luana Tanzi [a], Michele Nardone [a], Paola Benassi [a], Fabio Ramondo [a,*], Ruggero Caminiti [b], Lorenzo Gontrani [b,*]

[a] Department of Physical and Chemical Sciences, University of L'Aquila, Via Vetoio, I-67100, L' Aquila, Italy
[b] Department of Chemistry, University of Rome 'La Sapienza', P.le Aldo Moro 5, I-00185 Rome, Italy

ARTICLE INFO

Article history:
Received 6 October 2015
Accepted 7 February 2016
Available online xxxx

2010 MSC:
00-01
99-00

Keywords:
X-ray diffraction
Ab initio calculations
Molecular dynamics
Vibrational spectroscopy
Ionic liquids

ABSTRACT

We report here a combined experimental and theoretical study on the bio-compatible salicylate choline ionic liquid. The liquid structure has been investigated by X-ray diffraction and vibrational (IR and Raman) spectroscopy. Local structure has been obtained from *ab initio* calculations on static ion pairs and from dynamic simulations of a small portion of the liquid. The theoretical models indicate that salicylate is connected by hydrogen bonding to choline mainly through the carboxylate group and forms stable ion pairs. A strong intramolecular interaction hinders internal rotations of the OH group of salicylate and competes with the hydrogen bonding with choline. When the liquid has been simulated by classical force fields we found a good agreement with the X-ray experimental features, comparable to that obtained from AIMD simulations. Important insights on hydrogen bonding between carboxylate and choline have been also derived from the analysis of the CO stretching modes of carboxylate measured in the Raman and IR spectra and calculated from VDOS-Wannier centers procedures.

1. Introduction

Attention on ionic liquids (ILs) [1-3], molten salts at room temperature, is increasing day by day in science and technology. Among their unique characteristics like conductivity, polarity, chemical and thermal stability, nonflammability, the negligibly low vapor pressure is the fundamental feature to consider them as green solvent. The toxicity of a few ILs [4] lead to the development of ILs entirely composed of biomaterials (BioILs). They combine some of the excellent properties of traditional ILs with the advantage of bio-degradability, biocompatibility and non-toxicity. Their facile and green preparation, such as simple exchange and/or acid/base reactions [5], and the use of readily available and inexpensive starting materials, are further advantages of BioIls over ILs. The BioILs based on cholinium cation (2-hydroxyethyl)trimethylammonium coupled with a large variety of carboxylic acids of natural origin have found great interest [6]. Most studies on BioILs deal with their synthesis, their physical chemical properties [7-9] whereas few papers have studied their structure. Their important properties stem from the complexity of the interactions between molecular constituents, including long range Coulombic terms, short range van der Waals contributions along with anisotropic hydrogen bonding interaction. Recently infrared and Raman spectra [10] and X-ray studies [11] of three choline-based BioILs coupled with carboxylate anions have been reported and important structural features have been derived from classical and *ab initio* molecular dynamics. Furtherly, systems consisting of choline cation coupled with a series of amino acid anions have been investigated by X-ray diffraction [12,13], IR spectroscopy [12] and molecular dynamics [12-14]. All these studies [10-14] show that hydrogen bonding is a crucial feature in establishing the local geometric structure for these BIoILs.

Among choline-based BioILs, Yu et al. [15] synthesized choline benzoate and choline salicylate. From their density data [15] it was observed that they have molar volume lower than common ionic liquids and consequently they can moderately solubilize species like CO_2. Within this aim, a computational study has been carried out on these ionic liquids in the pure state and after CO_2 adsorption by classical and quantum chemical methods [16]. In order to characterize the structure of this class of choline-based ionic liquids by experiments, we present here a study of one member of the series, choline salicylate [Ch][Sal], in which we employ a combination of *ab initio* molecular dynamics (AIMD), classical molecular dynamics (MD) and experimental (X-ray diffraction, infrared and Raman spectroscopy) measurements with the aim of interpreting geometrical features and dynamic aspects of its structure. We have chosen a carboxylate anion, salicylate, able to form both intramolecular and intermolecular hydrogen bonding and it is interesting to compare its structure with that of systems where choline is coupled with simpler alkylcarboxylate anions [10,11]. The diffraction

* Corresponding authors.
E-mail addresses: fabio.ramondo@univaq.it (F. Ramondo), lorenzo.gontrani@uniroma1.it (L. Gontrani).

http://dx.doi.org/10.1016/j.molliq.2016.02.020
0167-7322/

patterns from measured X-ray and those from MD simulations can be compared to provide a validation of the theoretical models here applied.

Alternatively to X-ray studies, vibrational spectroscopy can be extremely useful for evaluating the nature of the cation–anion interactions, identifying ion pair coupling and clarifying conformational isomers [17-27]. For example, the presence and the force of hydrogen bonding may be obtained from the vibrational frequencies of the OH group of choline and the COO– group of carboxylate since directly involved in such interaction. On the other hand non-empirical AIMD simulations have been recently and successfully applied to a wide number of ionic liquids [28-32] to investigate their vibrational properties and assign the observed absorptions.

2. Experimental details

2.1. Synthesis

Reagents used in the synthesis were choline hydroxide solution (46 wt.% in H_2O, Aldrich) and salicylic acid(99%, Aldrich), both used without further purification. Choline salicylate was synthesized by dropwise addition of salicylic acid to the choline hydroxide solution in ratio 1:1 (*e.g.* 0.12 mol:0.12 mol), stirring continuously at room temperature and pressure for 12 h. Most of the water in the reaction mixture was removed under reduced pressure, using a rotary evaporator at 70 °C for 4 h. The mixture was then dried *in vacuo*, heating at 70 °C and stirring for 24 h. The purity of these BioILs was checked by 1H NMR and 13C NMR spectroscopy, using a Bruker Avance III spectrometer operating at 400 MHz and 100.6 MHz, respectively. The spectra have confirmed the absence of any major impurities and the water final content, evaluated by 1H NMR analysis, has been estimated below 0.4 wt.%.

2.2. X-ray scattering

The large angle X-ray scattering experiments were performed using the non-commercial energy-scanning diffractometer built in the Department of Chemistry at the University La Sapienza of Rome. (Patent no. 01126484— 23 June 1993). Detailed description of instrument, technique and the experimental protocol (instrument geometry and scattering angles) of the data acquisition phase can be found in a series of papers by our group [33-38]. The appropriate measuring time (*i.e.* number of counts) was chosen to obtain scattering variable (q) spectra with high signal to noise ratio (500,000 counts on average).

The expression of q is:

$$q = \frac{4\pi \sin(\theta)}{\lambda} = 1.014E \sin(\lambda) \tag{1}$$

where E is expressed in keV and q in $Å^{-1}$. The various angular data were processed according to the procedure described in literature [33-38], normalized to a stoichiometric unit of volume containing one ion pair and combined to yield the total (static) "structure factor", $I(q)$,

$$I(q) = I_{e.u.}(q) - \sum_{i=1}^{N} x_i f_i^2 \tag{2}$$

where f_i are the atomic scattering factors, x_i are the number concentrations of the i-type atoms in the stoichiometric unit (*i.e.* the group of particles used as reference for data normalization, the ion pair in this case) and $I_{e.u.}$ is the observed intensity in electron units (electrons^2).

Such function depends on the scattering contributions of all the particles of the system, according to the pairwise distances between them (in the case of X-rays, the atoms scatter the radiation through the electron clouds surrounding them) and therefore, it gives a sort of mathematical picture of the spatial disposition of the sample atoms. This function is multiplied by q and q-dependent sharpening factor, $M(q)$ (with nitrogen as sharpening atom) to enhance the resolution of the curve at high q values and to decrease the truncation error in the calculation of the Fourier transform from the reciprocal space (q) to the direct one (r). The expression for $M(q)$ is

$$M(q) = \frac{f_N^2(0)}{f_N^2(q)} exp(-0.01q^2) \tag{3}$$

Fourier transform of $qI(q)M(q)$ led to radial distribution function (r.d.f.)

$$D(r) = 4\pi r^2 \rho_0 + \frac{2r}{\pi} \int_0^{q_{max}} qI(q)M(q) \sin(rq)dq \tag{4}$$

where ρ_0 (electrons^2/Å^3) is the bulk number density. When the uniform distribution component is dropped ($4\pi r^2\rho_0$), we obtain the differential correlation function, *Diff*(r), which contains only the structural contribution to the distribution function,

$$Diff(r) = D(r) - 4\pi r^2 \rho_0 \tag{5}$$

2.3. Infrared and Raman spectra

The Fourier transformed infrared (FTIR) spectrum was measured at room temperature from 4000 to 400 cm^{-1} after 100 scans using the Perkin Elmer Spectrum two FT-IR spectrometer. Liquid samples were placed as thin films between KBr plates. The Raman spectrum was measured using a LABRAM confocal-microscope Raman spectrometer by HORIBA Jobin Yvon using 5 mW at 632 nm excitation source and a 20× collection optics. The instrumental resolution is of the order of 2–3 cm^{-1}. Background fluorescence has been fitted using a polynomial expression and subtracted from the data.

3. Computational details

3.1. Liquids by molecular dynamics

In order to describe the liquid structure we have followed two different approaches. Local structural characterization with particular attention to the hydrogen bonding interaction occurring between ion pairs was initially performed by *ab initio* methods.

Quantum-mechanical calculations on the choline–salicylate ion pair were performed using the Gaussian 09 package [39]. Equilibrium geometry and vibrational frequencies were obtained using Moller–Plesset (MP2) and density functional theory (DFT) methods with the B3LYP [40,41] exchange and correlation functional and employing the 6-311++G** basis set.

Dynamic effects were introduced at *ab initio* level by AIMD simulations performed on a model of 9 ion pairs using the Born–Oppenheimer Molecular Dynamics (BOMD) method implemented in the CP2K code [42]. Potential energy calculations were carried out using BLYP exchange-correlation functional [41,43] with the Grimme's dispersion correction D3 [44] and the hybrid Gaussian and plane wave (GPW) basis set [45]. Gaussian basis set was DZVP-MOLOPTSR-GTH and plane waves expansion was developed in a periodic cubic system with unit cell edge of 14.53 Å^3 and truncated at 320 Ry. Goedecker–Teter–Hutter (GTH) pseudopotentials [46,47] were employed to describe core electrons. A pre-equilibration was performed employing classical molecular dynamics within periodic boundary conditions using the two-body Generalized Amber Force Field (GAFF) [48]. AIMD simulations started from a snapshot of the classical MD simulation and the system was equilibrated for 6.3 ps in the NVT ensemble at 300 K using the individual thermostat for each degree of freedom for the first 3 ps and a global Nosé–Hooverchain thermostat [49-51] for the remaining time. Timestep was set to 0.4 fs. Trajectory was then collected for 20 ps in

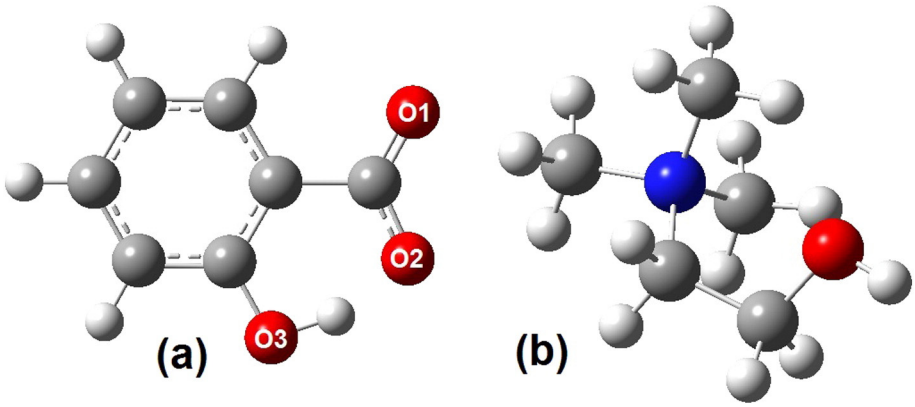

Fig. 1. Salicylate anion (a) and choline cation (b).

the NVT ensemble, saving velocities and coordinates every steps. During the production run, the Wannier centers [52] of the whole system have been evaluated at every sixth step in order to obtain the IR spectra.

In order to provide a full characterization of the liquid structure within the range of radial distances accessible to experiments we have performed a series of simulations with the previously cited (GAFF) using Gromacs v.4.6.2 package [53] as molecular dynamics engine. Simulations were carried out starting from partial atomic charges obtained using the Restrained Electrostatic Potential (RESP) method [54,55] by fitting the electrostatic potential for isolated cations and anions at the equilibrium geometry calculated at the HF/6-31G* level. The use of HF/6-31G* method has been demonstrated to lead to the implicit polarization required in the additive FF model of condensed phase systems, and complies with the rest of the GAFF parameter set, optimized to be compatible with the Cornell et al. families of Amber force fields [56] that implement this charge derivation scheme. Electrostatic interactions were calculated using Particle Mesh Ewald (PME) under periodic boundary conditions and Linear Constraint Solver (LINCS) algorithm was applied to all bonds involving hydrogen atoms. Cutoff radii for van der Waals and direct-space Ewald interactions were set to 10 Å. Parallelization was carried out with domain decomposition strategy and Message Passing Interface (MPI) paradigm.

Simulations have been performed on a cubic cell with edges of about 45 Å containing 300 ion pairs (CHSAL). Equilibration consisted in gradually heating the systems at 550 K in the NPT ensemble and then in cooling them to 300 K using Nosé–Hoover thermostat [49-51] and Parrinello–Rahman barostat [57-59] set to 1 atm. Equilibration time was about 1 ns and a relaxation period of 500 ps without barostat followed. Subsequently, the systems were simulated in NVT ensemble for 3.5 ns with integration time step of 2 fs and trajectories were collected every 1000 steps.

3.2. MD-derived structure factor

Molecular Dynamics allows us to calculate theoretical structure factors from pair correlation functions $g_{ij}(r)$. In fact, structure factor can be expressed with the following equation [60]

$$I(q) = \sum_{i=1}^{N} \sum_{j=1}^{N} x_i x_j f_i(q) f_j(q) H_{ij}(q) \tag{6}$$

in which $H_{ij}(q)$ are the partial structure factors, defined in terms of the pair correlation functions by the Fourier integral

$$H_{ij}(q) = 4\pi\rho_0 \int_0^{r_{max}} r^2 \left[g_{ij}(r) - 1\right] \frac{\sin(qr)}{qr} dr \tag{7}$$

where r_{max} is half the box edge. The partial structure factors and the theoretical total structure factor were calculated with an in-house written code. Theoretical $I(q)$ was then multiplied by q and the sharpening factor, $M(q)$, to obtain a theoretical $qI(q)M(q)$ function comparable with the experimental one. Theoretical $D(r)$ and $Diff(r)$ were calculated as described in the previous section for the experimental curves.

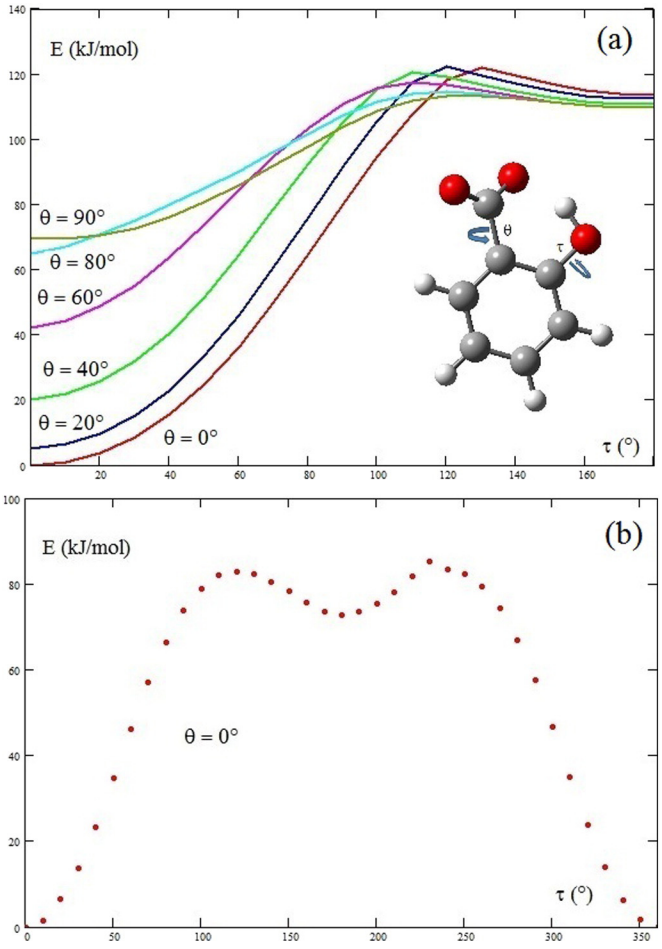

Fig. 2. (a) Scan of the dihedral angles θ and τ calculated for salicylate anion at the B3LYP/6–311++G** level; energies are calculated as $E(\theta, \tau) - E(\theta = 0^{\circ}, \tau = 0^{\circ})$. (b) Scan of the dihedral angle τ calculated for salicylate choline ion pair at the B3LYP/6–311++G** level; energies are calculated as $E(\tau) - E(\tau = 0^{\circ})$.

3.3. Vibrational spectra and assignment of vibrational modes

From static calculations on the ion pairs, vibrational frequencies and normal modes were computed by diagonalization of the Hessian matrix of the Potential Energy Surface (PES) at the equilibrium geometries. From the AIMD results, vibrational frequencies were obtained by analyzing the Vibrational Density of States (VDOS) [61,62]:

$$\mathrm{VDOS}(\omega) = \sum_{i=1}^{N} \int \langle \dot{r}_i(t)\dot{r}_i(0)\rangle \, exp(i\omega t)dt \tag{8}$$

Since VDOS is defined as sum of the Fourier transform of the atomic velocity autocorrelation functions (or power spectra), frequencies derived from such procedure include anharmonicity and temperature effects [62]. VDOS spectra can be decomposed into sum of power spectra of collective coordinates of the molecule q_k describing independent harmonic oscillations [61,62]:

$$VDOS(\omega) = \sum_{k,l} \int \langle \dot{q}_k(t)\dot{q}_l(0)\rangle \, exp(i\omega t)dt \tag{9}$$

The collective coordinates q_k are determined minimizing the functional $\Omega^{(n)}$:

$$\Omega^{(n)} = \sum_k \left[\frac{\beta}{\pi}\int d\omega |\omega^{2n}|P_k^q(\omega) - \left(\frac{\beta}{2\pi}\int d\omega |\omega^n|P_k^q(\omega)\right)^2\right] \tag{10}$$

where $P_k^q(\omega)$ is the power spectrum of k-th collective coordinate q_k and n is a fixed parameter, and imposing the decorrelation of vibrational normal modes and the equipartitioning of the energy as necessary conditions:

$$\frac{1}{2\pi}\int d\omega \int \langle \dot{q}_k(t)\dot{q}_l(0)\rangle \, exp(i\omega t)dt = \langle \dot{q}_k(t)\dot{q}_l(t)\rangle = k_B T\delta_{kl} \tag{11}$$

The minimization of functional $\Omega^{(n)}$ leads to an eigenvalue problem providing effective normal modes. We carried out minimization setting n = 2. For each effective normal mode, the power spectrum becomes localized in frequency [61,62].

4. Results and discussion

4.1. Ab initio static ion pair

Salicylate anion, Fig. 1(a), choline cation, Fig. 1(b) and choline salicylate ion pair were studied to investigate coupling geometry and structural changes due to association. Geometry optimizations reveal that the OH and COO– groups of salicylate interact through strong intramolecular hydrogen bonding both before and after association with choline.

The O–H distance, very short in isolated salicylate (1.452 Å B3LYP and 1.4295 Å MP2) suggests an easy intramolecular proton transfer. Such distance increases upon association with choline (1.641 Å B3LYP and 1.625 Å MP2) revealing that the choline coordination favors the localization of the proton on the OH group.

As for other carboxylate anions [10,11], interaction of choline with salicylate involves preferentially the COO– group for the presence of strong Coulombic interactions. Previous calculations [16] revealed that alternative structures, for example that where choline interacts with the OH group of salicylate, are remarkably less stable and therefore they were not considered in our study. The flexibility of the OH group of salicylate has been already tested through B3LYP/6–311++G** calculations of torsional barrier height on the salicylate anion by Aparicio [16]. Relaxed torsional scan has been here calculated again on the isolated anion by MP2/6–311++G** level confirming the high rotational barrier (about 90 kJ/mol). Simultaneous rotations of the COO– and OH groups have been further investigated at the B3LYP/6-311++G** level and Fig. 2(a) shows how the potential energy changes with the dihedral angles (θ and τ) which define the orientation of the substituents with respect to benzene ring. Results confirm that intramolecular

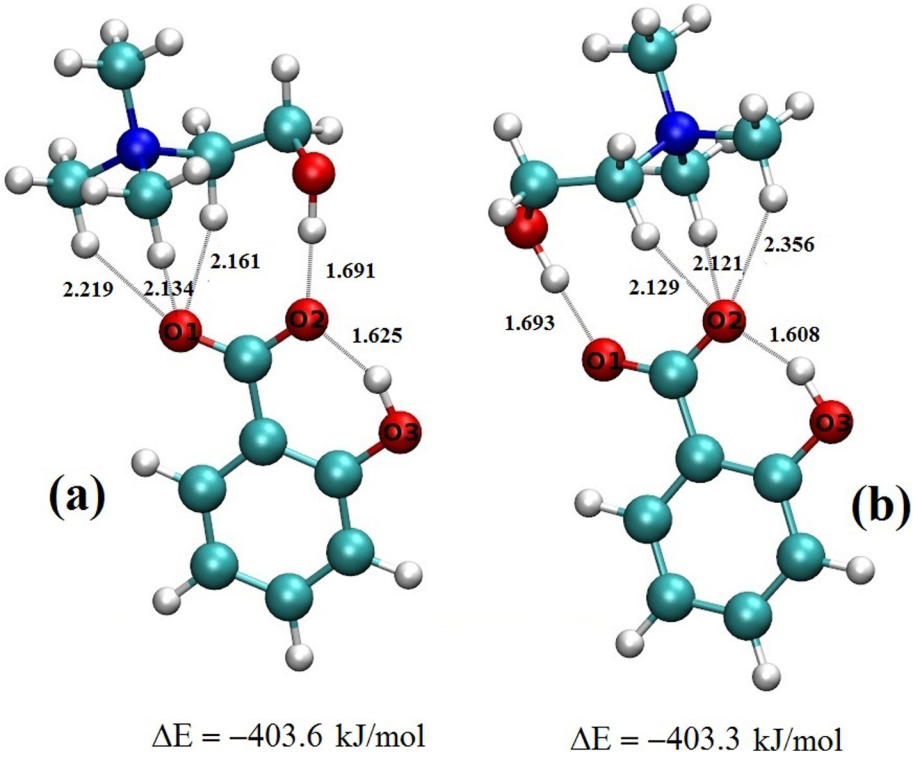

Fig. 3. The two stable *ab initio* ion pairs of [Ch][Sal]; the interaction distances (Å) and the interaction energies were obtained at the MP2/6–311++G** level.

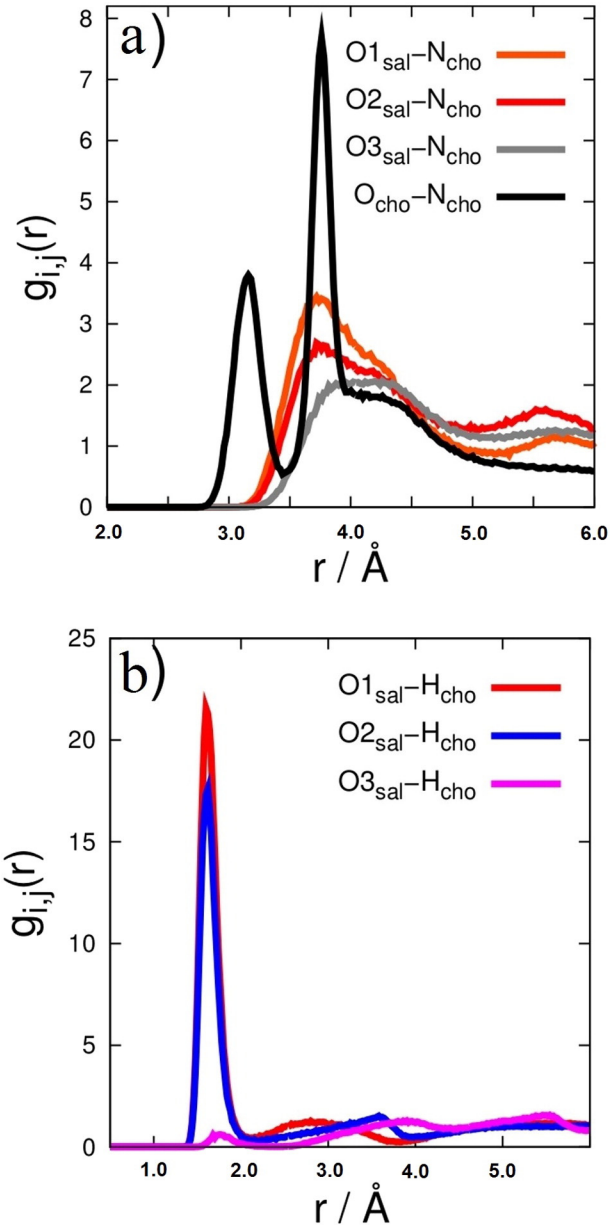

Fig. 4. RDFs of the oxygen–nitrogen distances (a) and RDFs of choline hydroxyl hydrogen atom and salicylate oxygen atoms (b).

hydrogen bonding is the main cause of stability of the equilibrium structure of salicylate anion. The OH rotational barrier height is in fact very high when carboxylate is coplanar to benzene ($\theta = 0°$) and therefore can form hydrogen bonding with OH group. A remarkable lowering of barrier height is instead expected when rotation of OH group is carried out by orienting the carboxylate in conformations which hinder intramolecular interactions (for example $\theta = 90°$). Consistently carboxylate is nearly free to rotate when the OH group assumes orthogonal orientation whereas it is rotationally hindered (70 kJ/mol) for coplanar orientation of the OH group. The OH barrier height has been calculated also for the salicylate choline ion pair and the results of Fig. 2(b) show that the OH torsion in salicylate is clearly hindered also in the presence of choline confirming that intramolecular hydrogen bonding is weakly affected by the cationic coordination.

Several coordination geometries were studied in the previous work [16] and the structure in which carboxylate forms simultaneously intra- and- inter-molecular hydrogen bonds through O_2 atom (see Fig. 3a) was found as the most stable ion pair. It's interesting to compare this structure with that of ion pairs where choline interacts with alkylcarboxylate anions, systems able to form only intermolecular interactions [10,11]. We notice that in salicylate hydrogen bonding with choline seems to be less stable due to competition between two hydroxyl groups: the hydrogen bond distance is about 1.7 Å whereas that in choline alkylcarboxylate pairs is within 1.6–1.7 Å. Among the alternative interaction geometries, we found a structure in which choline forms hydrogen bond with the other oxygen atom of carboxylate (O1), Fig. 3(b). The two structures together with geometries and interaction energies are shown in Fig. 3. Their stabilities, calculated at B3LYP and MP2, are indeed very similar (within 1 kJ/mol) suggesting that the potential around the carboxylate group is almost symmetrical and choline may interact with the oxygen atoms of the anion without any preference. Such structures were furtherly studied using the same plane wave basis set and the same functional, BLYP/GPW, employed for AIMD simulations. The hydrogen bond distances appear shorter (1.55 Å) than B3LYP and MP2 values (1.69 Å) however the binding energies of the two ion pairs are again very similar. We found only a slight preference for the structure O1–OH probably not significant. As already observed in choline alkylcarboxylate ion pairs [10,11], the coordination structure is also affected by secondary interactions CH–O as witnessed by some contacts between methyl hydrogen atoms and O1 or O2 atoms (see Fig. 3).

4.2. Classical molecular dynamics

Liquid structure was investigated through classical molecular dynamics. Despite classical force fields not always reproducing all the structural properties of protic ionic liquids [11,63], we decided to use anyway the GAFF force field, a modified AMBER force field which shares

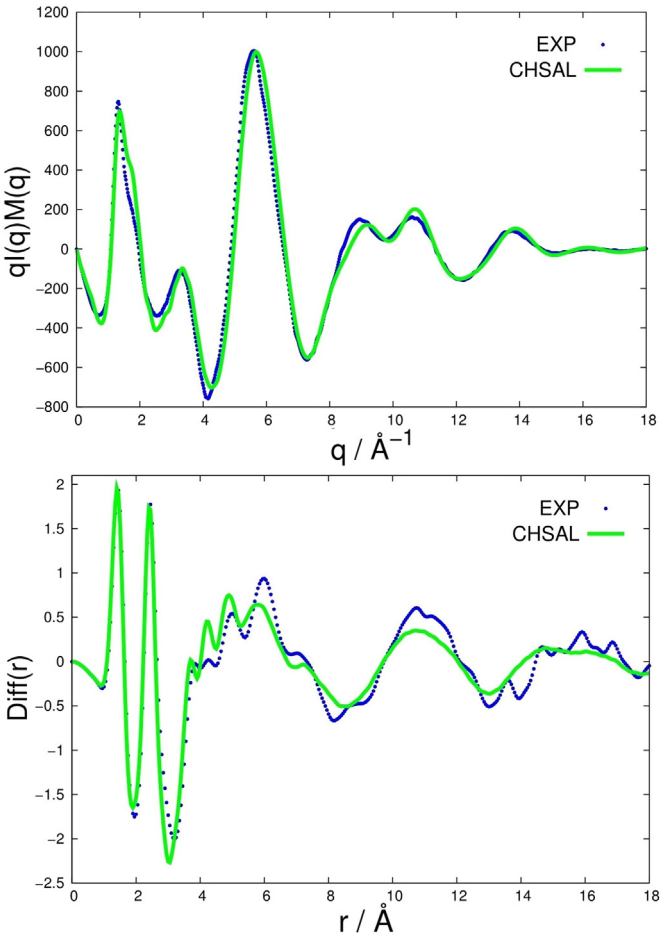

Fig. 5. Theoretical $qI(q)M(q)$ and $Diff(r)$ of CHSAL in comparison with experiment.

with it the same functional form to keep generality and transferability since it covers almost all the organic chemical space without need of further parameterization.

The structure of the single ionic component was initially analyzed through radial distribution functions of some intramolecular distances. Concerning anion, our simulations confirm the rigidity of the salicylate anion since no rotation occurs for both ring substituents. The distribution of the O–H distance is very narrow around O_2 and this is in agreement with the high OH rotational barrier height found from *ab initio* calculations and discussed above. On the other hand, the radial distribution function of Ncho–Ocho (Fig. 4a) allows us to investigate the distribution of gauche and anti-conformations of choline cation in liquid. Any variation of the NCCO dihedral angle changes the choline conformation and it affects the Ncho–Ocho distance. The two narrow peaks are associated to anti (3.8 Å) and gauche (3.2 Å) conformations and Fig. 4a reveals the presence of both the conformations with a small preference for the anti-structure. This is not entirely consistent with the *ab initio* results that predict an energetic preference for gauche conformations of isolated and coupled choline [10]. *Ab initio* geometry optimizations were carried out also in the present study for choline salicylate ion pairs starting from anti-conformation of choline and the results confirm the higher stability (about 16 kJ/mol) for the gauche orientation. However introducing a dielectric to simulate the bulk effect of the liquid is expected to lower the gauch-anti relative stability [10]. In addition we note that the choline conformation affects also the intermolecular hydrogen bonding since we calculated a O–H distance for the anti-conformation (1.782 Å) higher than that found for the gauche structure(1.694 Å).

The structuring of liquid was then analyzed by monitoring the radial distribution functions of some intermolecular distances. The narrow distribution of the O–H distances, Fig. 4(b), very similar to that found by Aparicio et al. [16], is a clear evidence that ions in liquid form very stable ion pairs. In the present study we attempted to separate the O_1 from O_2 atomic contribution in the O–H distance however both sites showed similar probability to form hydrogen bonding with a very small preference for O_1. The equivalence of the two hydrogen bonds is consistent with the fact that the carboxylate group has a nearly symmetric interaction potential in the classic force field here applied. The hydrogen bond distance (1.61 Å) is higher than that in alkylcarboxylate BioILs (1.55 Å) [11] and this is in agreement with *ab initio* results on the ion pair. Another important difference from alkylcarboxylate choline compounds is that the OH group of salicylate anions could give additional hydrogen bonds with choline cations. However the relative O3–H $_{cho}$ RDF shown in Fig. 4(b) reveals that this interaction plays a marginal role as already predicted from *ab initio* calculations.

The occurrence of anion–anion interactions, through the possible hydrogen bonding sites, as well as cation–cation interactions, through O–HO interactions, can be discarded on the light of the respective radial distribution functions and in agreement with the investigation of Aparicio et al. [16].

Radial distribution functions of intermolecular N–O_1 and N–O_2 distances are further shown in Fig. 4(a). It is interesting to observe that the distribution of such intermolecular distances occurs at values close to that of the N–O intramolecular distances of choline when it assumes anti-conformations. In the same region of the radial function another N–O distance is also expected, that due to O_3 atom, whose distribution is centered to a higher value. Therefore in the region between 3.5 Å and 4.5 Å we expect to observe a quite complex pattern originated by highly correlated intermolecular interactions (e.g. strong hydrogen

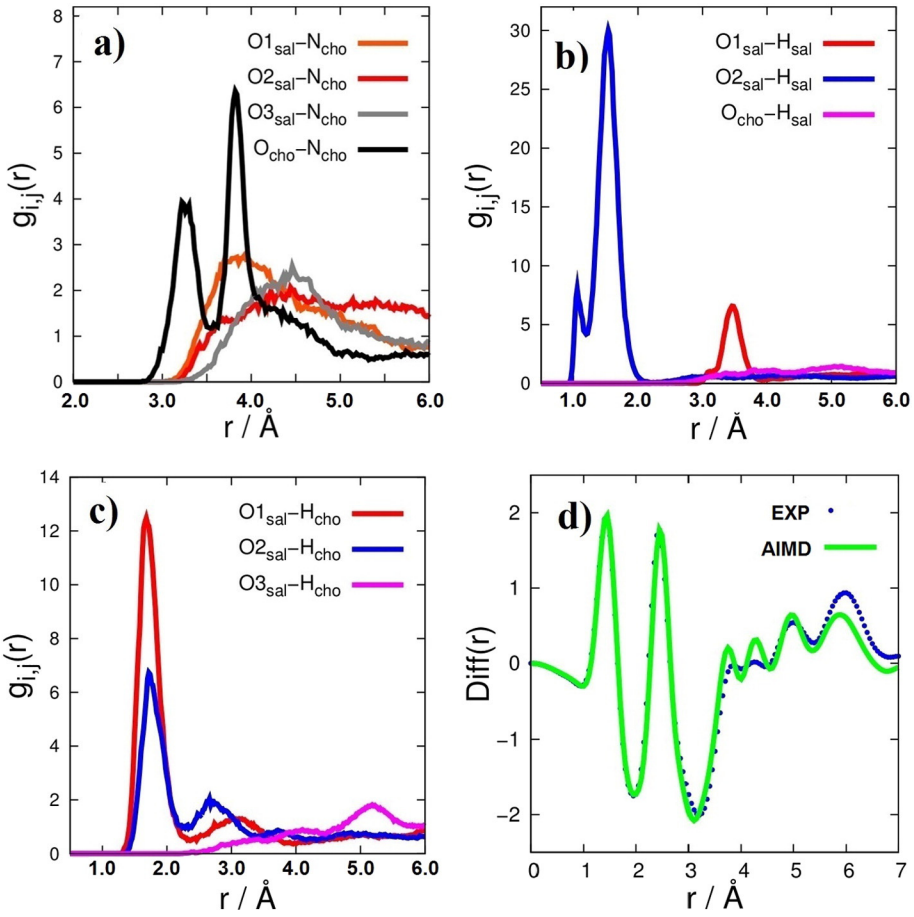

Fig. 6. Radial distribution functions of the oxygen–nitrogen distances (a). Radial distribution functions calculated between salicylate hydroxyl hydrogen and oxygen atoms (b) and between choline hydroxyl hydrogen and each salicylate oxygen atoms (c). AIMD Diff(r) in comparison with experiment (d).

bonds) along with intramolecular contacts between atoms with high scattering factors (e.g. N–O of choline).

In order to provide a validation of the theoretical results here presented, we have compared the findings from the MD simulations to the measured X-ray diffraction patterns. The structure function obtained from X-ray diffraction is reproduced in the upper panel of Fig. 5 and the complementary *Diff*(*r*) function is presented in the lower panel. In the same figure we present a comparison of the experimental curves with the function calculated from the MD simulations. We have a good agreement between the experimental and theoretical patterns on all range for both the curves. Both structure factors and differential correlation function follow experimental peak values and intensities in both intra- and inter-molecular structural ranges. On the basis of this agreement we can conclude that GAFF simulations provide a satisfactory description of choline salicylate liquid structure.

4.3. Ab initio molecular dynamics

A small portion of liquid was further studied by AIMD in order to validate the results of classical MD description. Although the *ab initio* MD approach is much more computationally demanding than classical MD and therefore it is often applied to small portion of liquids, it has the advantage to include, at least in principle, the exact interaction energy up to all the many body terms. The most important result here obtained is that some structural features emerging from the classical description are confirmed by *ab initio* simulations. For example the ring substituents in the salicylate anions are still conformationally rigid whereas in the choline cations a very small preference for anti-conformation is again found, Fig. 6(a). Other structural aspects can be better described by an *ab initio* approach. In particular intramolecular hydrogen bond, whose geometry in GAFF simulation was fixed by some empirical parameters of the force filed, can now be object of some considerations. Even if hydrogen continues to be mainly covalently bonded to O_3, as it just occurs in ion pair, during dynamics we can observe proton transfer from O_3 to O_2. Radial distribution function between O_2 and Hsal has in fact the main peak at values typical of very strong intramolecular hydrogen bonds (1.54 Å) along with an additional low intensity peak at the covalent bond distance of 1.06 Å, Fig. 6(b). The only remarkable difference between the two models is in the intermolecular hydrogen bond geometry: O_1 has a higher (near double) probability to bind choline with respect to O_2, as attested by the radial distribution function in Fig. 6(c); in addition O_1 forms hydrogen bonds (1.68 Å) slightly shorter than O_2 (1.72 Å). Thus AIMD simulations seem to reveal small asymmetries in the hydrogen bonding acceptor properties of two carboxylate oxygens not appreciable from zero temperature studies of ion pairs and from classical MD.

However this small structural differences do not drastically affect the theoretical differential correlation function, since it has a shape very similar to the GAFF *Diff*(*r*). The comparable nitrogen–oxygen distance distributions is probably one of the factor that contributes to this agreement, see Fig. 6(a). When compared with X-ray diffraction *Diff*(*r*) in Fig. 6(d), the AIMD curve gives good predictions of the experimental data in all the range considered as already observed for alkylcarboxylate choline liquids [11]. Both classical force field and *ab initio* models describe the choline salicylate as a liquid where cations and anions interact through hydrogen bonding weaker and less directional than that between choline and alkylcarboxylate components. As a consequence also a two-body potential as GAFF here applied, not particularly accurate for protic ionic liquids, reproduces satisfactorily the structural features of choline salicylate liquids.

4.4. Vibrational spectra

4.4.1. Ion pairs from quantum mechanical study

Vibrational spectra of choline cation, salicylate anion and choline salicylate ion pair were calculated from *ab initio* methods and frequencies of the groups involved in hydrogen bonding are reported in Table 1.

Table 1
Selected vibrational frequencies (cm^{-1}) of choline cation [Ch], salicylate anion [Sal] and their ion pair [Ch][Sal] at different levels of calculation.

	[Ch]		[Ch][Sal] Fig. 3(b)		[Ch][Sal] Fig. 3(a)	
	B3LYP	CP2K	B3LYP	CP2K	B3LYP	CP2K
Choline modes						
νOH $_{cho}$	3831	3664	3228	2893	3237	2957
δHOC $_{cho}$	1462	1415	1531	1531	1531	1523
νCO $_{cho}$	1101	1040	1114	1083	1113	1075
τCO $_{cho}$	314	300	918	956	931	951
	[Sal]					
Salicylate modes						
νOH	2357	2048	3168	2829	3187	2858
δHOC	1638	1596	1630/1668	1598	1627/1663	1587
νCO $_{sal}$	1262	1304	1278	1226	1283	1245
τCO	1103	1065	902	950	898	927
νCO $_{as}$	1704	1698	1604	1545	1598	1540
νCO $_{s}$	1340	1331	1368	1314	1371	1327
δOCO	815	820	812	797	809	795
γCOO	796	747	711	696	710	692
$\Delta\nu$OH $_{cho}$			603	771	594	707
$\Delta\nu$CO	364	367	236	231	227	213

As for alkylcarboxylate anions, the vibrational modes of carboxylate group can be classified as CO symmetric and CO asymmetric stretching vibrations and their frequencies differ each other, $\Delta\nu$CO, by about 364 cm^{-1} a value not far from those observed for the group in other carboxylate anions (324–309 cm^{-1}) [10]. In the benzoate anion, where the carboxylate group is rigorously symmetric, such difference is calculated at 338 cm^{-1}. As for alkylcarboxylate choline ion pairs [10], hydrogen bonding between cation and anion is expected to change the CO vibrational coordinates and consequently their frequencies. In addition such changes, expressed for example again as difference between the symmetric and asymmetric stretching frequencies, $\Delta\nu$CO, can be correlated with the strength of the intermolecular interaction [10]. In our case the frequencies of Table 1 indicate that CO–HO hydrogen bonding causes a marked decrease of $\Delta\nu$CO from 365 cm^{-1} (isolated anion) to about 230 cm^{-1} (coupled anion). In addition it's worth noting that $\Delta\nu$CO of salicylate choline is similar to that of formate (250 cm^{-1}), but higher than those of propanoate (175 cm^{-1}) and butanoate (184 cm^{-1}) choline suggesting a hydrogen bonding weaker than alkylcarboxylate choline ion pairs [10]. The strength of ion pairing can be evaluated more easily following the modes of the choline cation. Table 1 shows that the red shift of the OH stretching frequency ($\Delta\nu$OH) (about 600 cm^{-1}) and the blue-shift of torsion frequency ($\Delta\tau$CO) (about 600 cm^{-1}) are smaller than those of alkylcarboxylate choline, 750 and 650 cm^{-1}, respectively,

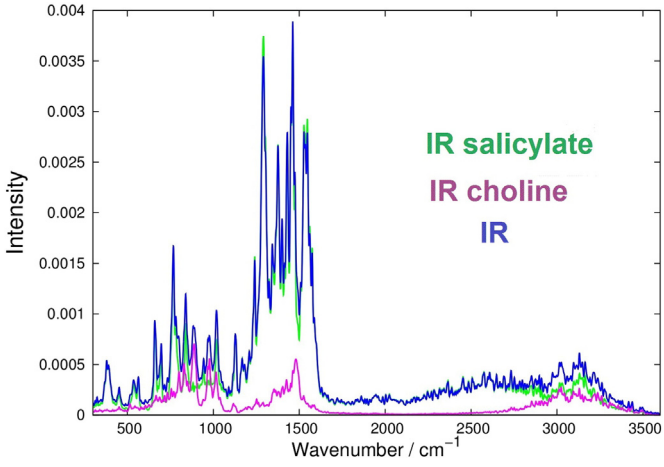

Fig. 7. Infrared spectrum of [Ch][Sal] and its components.

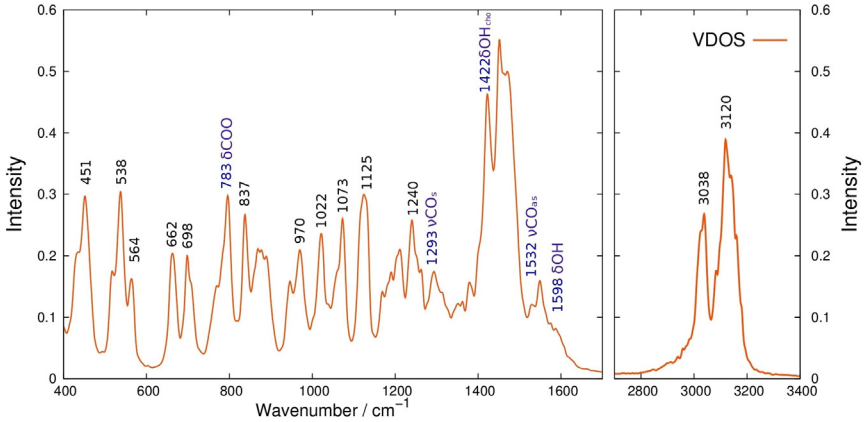

Fig. 8. VDOS spectrum of [Ch][Sal].

confirming that intermolecular hydrogen bond is weaker in choline salicylate.

Table 1 shows also the frequencies and their shifts calculated from CP2K method. The values are quite different from the B3LYP/6–311++G** ion pair and in particular the BLYP/GPW level used for CP2K calculations enhances the frequency shifts of the hydroxyl modes. $\Delta\nu$CO is instead less affected by the calculation level. Interesting is also the comparison between the two ion pairs in which salicylate forms intermolecular hydrogen bond respectively through O_1 and O_2 atoms. Notwithstanding the geometries of the two structures suggest that when interaction involves O_1 intra- and inter-molecular hydrogen bonding is stronger, the OH choline stretching undergoes shifts very similar in agreement with their close stability. Only at the BLYP/GPW level the $\Delta\nu$OH values are slightly different and that for O1–HO interaction is higher. We can also notice that in the both interaction models the OH stretching coordinates of choline and salicylate are significantly coupled.

4.4.2. AIMD spectra

The computation of Wannier centers during AIMD simulation allows to obtain a theoretical IR spectrum. An advantage of the simulated spectrum is the possibility to split it into its cationic and anionic components: Fig. 7 shows the total IR spectrum and the partial IR spectra.

At first sight, we note that the total IR spectrum is largely dominated by the intense bands of salicylate: choline has bands with comparable intensities only in the low 500–1100 cm^{-1} and high 2800–3400 cm^{-1} frequency ranges. Beyond these regions, IR spectrum can be easily assigned since all bands belong exclusively to salicylate, on the contrary, inside this range there are overlapping bands.

In analogy to harmonic frequencies and normal mode analysis, vibrational frequencies and effective normal modes can be obtained from a VDOS decomposition, as displayed by the works of Martinez [61,62]. Using this technique, dynamical solvation, temperature and anharmonicity effects are directly and explicitly taken into account in the vibrational frequencies and normal modes (Fig. 8). The comparison with frequencies of ion pairs calculated at the same theoretical level (CP2K) reveals that finite temperature weakens intermolecular hydrogen bonding and strengthens the intramolecular one. For example the OH group of salicylate is involved in very stable hydrogen bonding, and probably its chemical environment does not change its conformational rigidity so much. For this reason, salicylate OH bending shows frequency similar to ion pair. On the contrary, the OH bending of choline is more affected by the intermolecular environment and its frequency lowers from the ion pair to AIMD models. Regarding the CH and OH stretching frequency range, while the former are rather well localized, the OH vibrations are distributed on a very broad range and their mean value cannot be calculated with high accuracy from VDOS spectrum. This is a consequence of the wide distribution of hydrogen bonding energies and conformations that is typical of protic liquids. Despite the scarce localization, the power spectra still indicate that two hydroxyl groups of [Ch][Sal] form hydrogen bonding of different strength: power spectra for choline distribute around a mean value of 3240 cm^{-1}, whereas for salicylate the mean value is 2655 cm^{-1}, lower than ion pairs.

4.4.3. Experimental IR and Raman spectra

Vibrational properties of liquid [Ch][Sal] were experimentally studied through IR and RAMAN spectra (Fig. 9).

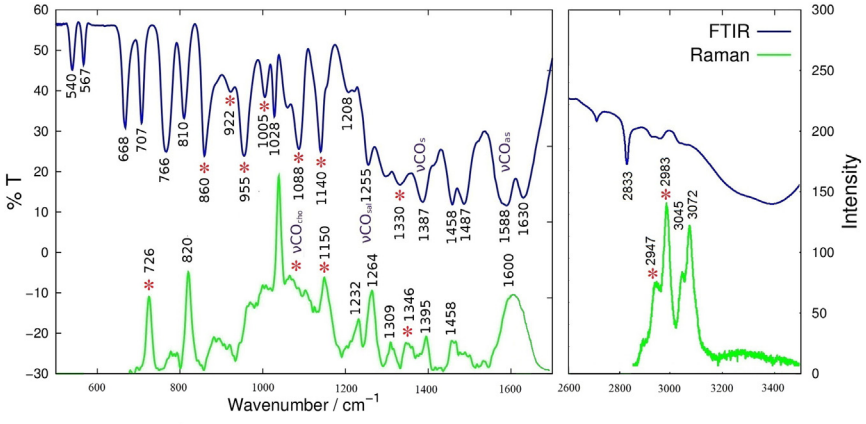

Fig. 9. Infrared and Raman spectrum of [Ch][Sal]. Bands of choline are marked with a star.

Table 2
Experimental IR and Raman frequencies (cm^{-1}) of choline salicylate liquid and theoretical frequencies from AIMD and [Ch][Sal] ion pair (CP2K).

	IR	Raman	AIMD	CP2K
Choline modes				
νOH $_{cho}$	3400–3200			2957
νCH $_{cho}$		2983		3147
νCH $_{cho}$		2947	3038	3123–2931
δHOC $_{cho}$			1422	1523
ρCH3	1330	1346		1275
ρCH3	1140	1150		1145–1138
νCO $_{cho}$	1088	1090		1075
νCC	1005		1022	973
τCO $_{cho}$	955		970	951
νCN	860			861–810
Salicylate modes				
νCH		3072		3196–3185
νCH		3045	3120	3144
νOH	2833			2858
νC═C	1630	1600	1550	1634
νCO $_{as}$	1588	1600	1532	1540
δHOC			1598	1587
νC═C	1487	1490	1480	1488
νC═C	1458	1458	1460	1461
νCO $_{s}$	1387	1395	1293	1327
νCO $_{sal}$	1255	1264	1240	1245
δCH	1208	1232	1200	1203–1213
δCH + νCC	1028	1035	1022	1030
δOCO	810	820	837	795
γCH	766	770	783	742
γCOO	707			685/691
δCCC	668		698	669
δCCC	567		564	612
γCCC	540		538	531

Assignment of the main peaks is reported in Table 2 and it is based on the theoretical results discussed above and on the experimental spectra of the two components.

Choline bands were already measured in alkylcarboxylate choline liquids [10] or in systems where choline is weakly coupled with anions [64] and we find them substantially unchanged in our liquid (see Fig. 9). On the other hand IR and Raman spectra of salicylate complexes in water solutions are very handful to assign the anionic bands [65,66]. As we have seen from the AIMD IR spectrum of choline salicylate liquid, the region over 1200 cm^{-1} is mainly dominated by salicylate bands although the assignment of all the observed peak is not easy. Regarding the higher frequency range (>2000 cm^{-1}), the Raman spectrum shows the band of CH stretching of choline cation (2983–2947 cm^{-1}) and salicylate anion (3072–3045 cm^{-1}), well localized and satisfactorily predicted in the VDOS spectrum. The OH stretching vibration of choline presents a broad IR absorption between 3200 and 3400 cm^{-1} owing to the wide distribution of intermolecular hydrogen bonds and choline conformations. On the contrary, the OH group of salicylate, involved in a strong intramolecular hydrogen bonding and conformationally quite rigid, is expected at lower frequency and it gives the sharp IR peak at 2833 cm^{-1}.

The frequencies calculated at 1634, 1587 and 1540 cm^{-1} are a mixture between benzene ring stretching modes, the bending of the OH group and the asymmetric vibration of the carboxylate group. From the analysis of normal modes the highest frequency, 1634 cm^{-1}, seems to be more characteristic of C═C stretching and it well compares with the IR absorption at 1630 cm^{-1}. The other strong IR bands at 1588 cm^{-1} can be assigned to the asymmetric carboxylate stretching. In this region the Raman spectrum shows a strong and quite large band at about 1600 cm^{-1}. The other important vibration, the OH salicylate bending, is predicted at 1587 cm^{-1}, from ion pair model and at 1598 cm^{-1}, from AIMD simulations, in a zone where broad absorptions are measured in the IR and Raman spectra. The OH group of choline cations is expected to have a bending mode at lower frequency, 1523 cm^{-1} (ion-pair) and 1422 cm^{-1} (AIMD), not easily observable in the measured spectra. In this region we observe two IR intense peaks at 1487 cm^{-1} and 1458 cm^{-1}, typical of phenol ring stretching modes, less pronounced in the Raman spectrum and well reproduced by AIMD simulations.

At lower frequency, the strong IR absorption at 1387 cm^{-1} can be assigned to the carboxylate symmetric stretching and the corresponding Raman band is found at 1395 cm^{-1}. The C–O stretching modes of two hydroxyl groups, νCO $_{cho}$ and νCO $_{sal}$, are identified with the strong absorptions at 1088 (IR)/1090(Raman) cm^{-1} (choline) and 1255 (IR)/1264(Raman) cm^{-1} (salicylate). This mode seems to be not strongly affected by chemical environment since the peak at 1088 cm^{-1} is observed in all choline based ILs spectra [10]. Some of the bands measured at the lower frequency have been assigned as reported in Table 2.

In Table 3 the values of νCO measured for some ionic liquids are compared with those of the same anions measured in different phases, from gas-phase [67,68], sodium salts [69,70] to water solution [66,69,71]. $\Delta\nu$CO for gas-phase carboxylate anions, well reproduced by our DFT calculations, decrease in condensed phase, in agreement with our results. In addition $\Delta\nu$CO for BioILs are comparable to those in water, suggesting that hydrogen bonding between ions in these liquids is fundamental as hydrogen bonding between carboxylate anions and water.

Table 3
$\Delta\nu$CO (cm^{-1}) of some carboxylate anions observed in condensed and gas phases and calculated from DFT theory.

	Gas Phase		Condensed Phase				
	Exp	B3LYP	Water	Na salts	Ionic Liquids	Ion pair (B3LYP)	AIMD
Formate		324[a]	229[b]	201[c]	255[a]	251[a]	263[a]
Acetate	285[d]	303[d]	135[b]	162[c]		182[e]	
Propionate	295[d]	305[a]	132[b]	136[c]	161[a]	175[a]	236[a]
Butanoate		309[a]	135[b]	173[c]	140[a]	184[a]	201[a]
Benzoate	315[f]	338[e]	155[g]	143[g]		197[e]	
Salicylate		364[e]	207[h]		201[e]	227[e]	239[e]

[a] Ref. [10].
[b] Ref. [71].
[c] Ref. [69].
[d] Ref. [67].
[e] This work.
[f] Ref. [68].
[g] Ref. [70].
[h] Ref. [66].

5. Conclusions

We have reported in this work energy dispersive X-ray diffraction data and IR and Raman spectra for a bio-compatible ionic liquid formed by choline cations and salicylate anions. Different theoretical models have been proposed to describe the liquid and the results have been compared with the experiments. Quantum mechanical approaches have been followed to describe the liquid structure: single ion pairs and small portions of liquid have been modeled by *ab initio* calculations and the results indicate that the ions are connected by strong hydrogen bonds. Salicylate has different hydrogen bonding acceptor groups however the theoretical models indicate that salicylate is connected by choline mainly through the carboxylate group. The X-ray pattern has been successfully reproduced by *ab initio* MD simulations within the obvious spatial and temporal limits of the employed model. Despite classical force fields do not reproduce always all the observed structural features of protic ionic liquids, in the present case the MD simulations obtained with the GAFF potential give structure function and the complementary *Diff*(*r*) one in good agreement with the X-ray patterns. Both AIMD and MD simulations give the choline proton sharply localized around the oxygen atoms of carboxylate and the acceptor–donor distance slightly higher than in alkylcarboxylate choline liquids. An important difference with respect to alkylcarboxylate choline liquid is that in salicylate based

liquids we found an intramolecular interaction quite strong which hinders internal rotations of the OH group of salicylate and competes with intermolecular hydrogen bonding. This intramolecular interaction is maintained in gas and liquid phases and its force is weakly affected by the choline coordination. The competition between the choline OH and salicylate OH groups over carboxylate weakens the strong directional character of intermolecular hydrogen bonding, one of the causes of failure of the classical force field in describing protic ionic liquids. AIMD simulations have been also used to model the measured absorption infrared spectrum of the liquid through VDOS-Wannier center calculations. In the VDOS spectra we can clearly identify the CH stretching vibrations, appearing as quite narrow bands and in agreement with the Raman absorptions, and separate them from the large absorption due to vibrations of the hydrogen bonded OH choline group. The band of the OH salicylate group is instead better localized in the VDOS spectrum in agreement with its strong intramolecular hydrogen bonding. Additional insights of hydrogen bonding between carboxylate and choline have been obtained from the analysis of the CO stretching modes of carboxylate measured in the Raman and IR spectra.

Acknowledgments

We acknowledge the CINECA award under the ISCRA initiative, for the availability of high performance computing resources and support, grant DYNGEOM. The authors also thank Professor Ruggero Caminiti (Department of Chemistry, Rome Sapienza University) for providing free computing time on NARTEN Cluster HPC Facility.

References

[1] J.S. Wilkes, A short history of ionic liquids from molten salts to neoteric solvents, Green Chem. 4 (2002) 73–80.
[2] E.W. Castner Jr., J.F. Wishart, Spotlight on ionic liquids, J. Chem. Phys. 132 (2010) 120901–120909.
[3] P. Wasserscheid, W. Keim, Ionic liquids: new solutions for transition metal catalysis, Angew. Chem. Int. Ed. 39 (2000) 3772–3789.
[4] N. Gathergood, P. Scammells, M. García, Biodegradable ionic liquids part III. The first readily biodegradable ionic liquids, Green. Chem. 8 (2006) 156–160.
[5] M. Petkovic, K.R. Seddon, L.P.N. Rebelo, C.S. Pereira, Ionic liquids: a pathway to environmental acceptability, Chem. Soc. Rev. 40 (2011) 1383–1403.
[6] Y. Fukaya, Y. Iizuka, K. Sekikawa, H. Ohno, Bio ionic liquids: room temperature ionic liquids composed wholly of biomaterials, Green Chem. 9 (2007) 1155–1157.
[7] N. Muhammad, M.I. Hossain, Z. Man, M. El-Harbawi, M.A. Bustam, Y.A. Noaman, N.B.M. Alitheen, M.K. Ng, G. Hefter, C.Y. Yin, Synthesis and physical properties of choline carboxylate ionic liquids, J. Chem. Eng. Data 57 (2012) 2191–2196.
[8] J. Restolho, J.L. Mata, B. Saramago, Choline based ionic liquids: interfacial properties of RTILs with strong hydrogen bonding, Fluid Phase Equilib. 322-323 (2012) 142–147.
[9] R. Klein, H. Dutton, O. Diat, G.J.T. Tiddy, W. Kunz, Thermotropic phase behavior of choline soaps, J. Phys. Chem. B 115 (2011) 3838–3847.
[10] L. Tanzi, P. Benassi, M. Nardone, F. Ramondo, Vibrations of bioionic liquids by ab initio molecular dynamics and vibrational spectroscopy, J. Phys. Chem. A 118 (2014) 12229–12240.
[11] L. Tanzi, F. Ramondo, R. Caminiti, M. Campetella, A.D. Luca, L. Gontrani, Structural studies on choline-carboxylate bio-ionic liquids by X-ray scattering and molecular dynamics, J. Chem. Phys. 134 (2015) 114506–114510.
[12] M. Campetella, E. Bodo, R. Caminiti, A. Martino, F. D'Apuzzo, S. Lupi, L. Gontrani, Interaction and dynamics of ionic liquids based on choline and amino acid anions, J. Chem. Phys. 142 (2015) 234502–234510.
[13] M. Campetella, S.D. Santis, R. Caminiti, P. Ballirano, C. Sadun, L. Tanzi, L. Gontrani, Is a medium-range order pre-peak possible for ionic liquids without an aliphatic chain? RSC Adv. 5 (2015) 50938–50941.
[14] A. Benedetto, E. Bodo, L. Gontrani, P. Ballone, R. Caminiti, Amino acid anions in organic ionic compounds. an ab initio study of selected ion pairs, J. Phys. Chem. B 118 (2014) 2471–2486.
[15] Y. Yu, X. Lu, Q. Zhou, K. Dong, H. Yao, S. Zhang, Biodegradable naphthenic acid ionic liquids: synthesis, characterization, and quantitative structure-biodegradation relationship, Chem. Eur. J. 114 (2008) 11174–11182.
[16] S. Aparicio, M. Atilhan, A computational study on choline benzoate and choline salicylate ionic liquids in the pure state and after CO_2 adsorption, J. Phys. Chem. B 116 (2012) 9171–9185.
[17] R.W. Berg, Raman spectroscopy and ab-initio model calculations on ionic liquids, Monatsh. Chem. 138 (2007) 1045–1075.
[18] M.J. Monteiro, F.C.C. Barito, L.J.A. Siqueira, M.C.C. Ribeiro, R.M. Torresi, Transport coefficients, Raman spectroscopy, and computer simulation of lithium salt solutions in an ionic liquid, J. Phys. Chem. B 112 (2008) 2102–2109.
[19] J.C. Lassegues, J. Grandin, D. Cavagnat, P.J. Johansson, New interpretation of the CH stretching vibrations in imidazolium-based ionic liquids, J. Phys. Chem. A 113 (2009) 6419–6421.
[20] M.C.C. Ribeiro, High viscosity of imidazolium ionic liquids with the hydrogen sulfate anion: a Raman spectroscopy study, J. Phys. Chem. B 116 (2012) 7281–7290.
[21] E. Bodo, P. Postorino, S. Mangialardo, G. Piacente, F. Ramondo, F. Bosi, P. Ballirano, R. Caminitii, Structure of the molten salt methyl ammonium nitrate explored by experiments and theory, J. Phys. Chem. B 115 (2011) 13149–13161.
[22] E. Bodo, S. Mangialardo, F. Ramondo, F. Ceccacci, P. Postorino, Unravelling the structure of protic ionic liquids with theoretical and experimental methods: ethyl-, propyl- and butylammonium nitrate explored by Raman spectroscopy and DFT calculations, J. Phys. Chem. B 116 (2012) 13878–13888.
[23] C.M. Burba, N.M. Rocher, R. Frech, hydrogen-bonding and ion-ion interactions in solutions of triflic acid and 1-ethyl-3-methylimidazolium triflate, J. Phys. Chem. B 113 (2009) 11453–11458.
[24] C.M. Burba, J. Janzen, E.D. Butson, G.L. Coltrain, Using FT-IR spectroscopy to measure charge organization in ionic liquids, J. Phys. Chem. B 117 (2013) 8814–8820.
[25] H.K. Stassen, R. Ludwig, A. Wulf, J. Dupont, Imidazolium salt ion pairs in solution, Chem. Eur. J. 21 (2015) 8324–8335.
[26] D. Paschek, B. Golub, R. Ludwig, Hydrogen bonding in a mixture of protic ionic liquids: a molecular dynamics simulation study, Phys. Chem. Chem. Phys. 17 (2015) 8431–8440.
[27] K. Fumino, A. Bonsa, B. Golub, D. Paschek, R. Ludwig, Non-ideal mixing behaviour of hydrogen bonding in mixtures of protic ionic liquids, ChemPhysChem 16 (2015) 299–304.
[28] M. Brehm, H. Weber, A.S. Pensado, A. Stark, B. Kirchner, Proton transfer and polarity changes in ionic liquid-water mixtures: a perspective on hydrogen bonds from ab initio molecular dynamics at the example of 1-ethyl-3-methylimidazolium acetate-water mixtures-part 1, Phys. Chem. Chem. Phys. 14 (2012) 5030–5044.
[29] K. Wendler, M. Brehm, F. Malberg, B. Kirchner, L. Delle Site, Short time dynamics of ionic liquids in aimd-based power spectra, J. Chem. Theory Comput. 8 (2012) 1570–1579.
[30] E. Bodo, A. Sferrazza, R. Caminiti, S. Mangialardo, P. Postorino, A prototypical ionic liquid explored by ab initio molecular dynamics and Raman spectroscopy, J. Chem. Phys. 139 (2013) 144309–144316.
[31] M. Thomas, M. Brehm, O. Hollóczki, Z. Kelemen, L. Nyĺaszi, T. Pasinszki, B. Kirchner, Simulating the vibrational spectra of ionic liquid systems: 1-ethyl-3-methylimidazolium acetate and its mixtures, J. Chem. Phys. 141 (2014) 24510–24520.
[32] M. Thomas, M. Brehm, R. Fligg, P. Vohringer, B. Kirchner, Computing vibrational spectra from ab initio molecular dynamics, Phys. Chem. Chem. Phys. 15 (2013) 6608–6622.
[33] L. Gontrani, F. Ramondo, R. Caminiti, Furan and thiophene in liquid phase: an X-ray and molecular dynamics study, Chem. Phys. Lett. 417 (2006) 200–205.
[34] L. Gontrani, F. Ramondo, G. Caracciolo, R. Caminiti, A study of cyclohexane, piperidine and morpholine with X-ray diffraction and molecular simulations, J. Mol. Liq. 139 (2007) 23–28.
[35] L. Gontrani, R. Caminiti, L. Bencivenni, C. Sadun, Molecular aggregation phenomena in solution: an energy dispersive X-ray diffraction study of concentrated imidazole water solution, Chem. Phys. Lett. 301 (1999) 131–137.
[36] R. Caminiti, M. Carbone, C. Sadun, Palladium (II) and platinum (II) aqueous solutions. evidence for the solvation of the $[PdCl_4]_2$ and $[PtCl_4]_2$ ions, J. Mol. Liquid. 75 (1998) 149–158.
[37] M. Carbone, R. Caminiti, C. Sadun, Structural study by energy dispersive X-ray diffraction of amorphous mixed hydroxycarbonates containing Co, Cu, Zn, Al, J. Mat. Chem. 6 (1996) 1709–1716.
[38] L. Gontrani, O. Russina, F.C. Marincola, R. Caminiti, An energy dispersive X-ray scattering and molecular dynamics study of liquid dimethyl carbonate, J. Chem. Phys. 131 (2009) 244503–244509.
[39] M.J. Frisch, G.W. Trucks, H.B. Schlegel, G.E. Scuseria, M.A. Robb, J.R. Cheeseman, G. Scalmani, V. Barone, B. Mennucci, G.A. Petersson, et al., Gaussian 09, Revision C.01, Gaussian Inc., Wallingford CT, 2010.
[40] A.D. Becke, Density functional thermochemistry. III. The role of exact exchange, J. Chem. Phys. 98 (1993) 5648–5652.
[41] C. Lee, W. Yang, R. Parr, Development of the colle-salvetti correlation energy formula into a functional of the electron density, Phys. Rev. B 37 (1988) 785–789.
[42] J. Hutter, M. Iannuzzi, F. Schiffmann, J. VandeVondele, Cp2k: atomistic simulations of condensed matter systems, Comput. Mol. Sci. 4 (2014) 15–25.
[43] A.D. Becke, Density-functional exchange-energy approximation with correct asymptotic behavior, Phys. Rev. A 38 (1988) 3098–3100.
[44] S. Grimme, J. Antony, S. Ehrlich, H. Krieg, A consistent and accurate ab initio parametrization of density functional dispersion correction (DFT-D) for the 94 elements H–Pu, J. Chem. Phys. 132 (2010) 154104–154119.
[45] H.T. Schaef, J.S. Loring, V.A. Glezakou, Q.R. Miller, J. Chen, A.T. Owen, M.S. Lee, E.S. Ilton, A.R. Felmy, B.P. McGrail, C.J. Thompson, Quickstep: fast and accurate density functional calculations using a mixed gaussian and plane waves approach, J. Comput. Chem. Commun. 167 (2005) 103–128.
[46] S. Goedecker, M. Teter, J. Hutter, Separable dual-space Gaussian pseudopotentials, Phys. Rev. B 54 (1996) 1703–1710.
[47] S.G.C. Hartwigsen, J. Hutter, Relativistic separable dual-space gaussian pseudopotentials from h to rn, Phys. Rev. B 58 (1998) 3641–3662.
[48] J. Wang, R. M. Wolf, J. W. Caldwell, P. A. Kollamn, D. A. Case, Development and testing of a general amber force field, J. Comput. Chem. 25 (2004) 1157–1174.
[49] S. Nosé, A unified formulation of the constant temperature molecular dynamics methods, J. Chem. Phys. 81 (1984) 511–519.
[50] S. Nosé, A molecular dynamics method for simulations in the canonical ensemble, Mol. Phys. 52 (1984) 255–268.

[51] W.G. Hoover, Canonical dynamics: equilibrium phase-space distributions, Phys. Rev. A 31 (1985) 1695–1697.
[52] N. Marzari, D. Vanderbilt, Maximally localized generalized wannier functions for composite energy bands, Phys. Rev. B 56 (1997) 12847–12865.
[53] E. Lindahl, B. Hess, D. van der Spoel, Gromacs 3.3; a package for molecular simulation and trajectory analysis, J. Mol. Mod. 7 (2001) 306–317.
[54] W.D. Cornell, P. Cieplak, C.I. Bayly, P.A. Kollman, Application of resp charges to calculate conformational energies, hydrogen bond energies, and free energies of solvation, J. Am. Chem. Soc. 115 (1993) 9620–9631.
[55] P. Cieplak, W.D. Cornell, C.I. Bayly, P.A. Kollman, Application of the multimolecule and multiconformational resp methodology to biopolymers: charge derivation for DNA, RNA, and proteins, J. Comput. Chem. 16 (1995) 1357–1377.
[56] W.D. Cornell, P. Cieplak, C.I. Bayly, I.R. Gould, K.M. Merz Jr., D.M. Ferguson, D.C. Spellmeyer, T. Fox, J.W. Caldwell, P.A. Kollman, A second generation force field for the simulation of proteins, nucleic acids, and organic molecules, J. Am. Chem. Soc. 117 (1995) 5179–5197.
[57] M. Parrinello, A. Rahman, Crystal structure and pair potentials: a molecular-dynamics study, Phys. Rev. Lett. 45 (1980) 1196–1199.
[58] M. Parrinello, A. Rahman, Polymorphic transitions in single crystals: a new molecular dynamics method, J. Appl. Phys. 52 (1981) 7182–7190.
[59] G.J. Martyna, D.J. Tobias, M.L. Klein, Constant pressure molecular dynamics algorithms, J. Chem. Phys. 101 (1994) 4177–4189.
[60] C.J. Pings, J. Waser, Analysis of scattering data for mixtures of amorphous solids or liquids, J. Chem. Phys. 48 (1968) 3016–3018.
[61] M. Martinez, M.-P. Gaigeot, D. Borgis, R. Vuilleumier, Extracting effective normal modes from equilibrium dynamics at finite temperature, J. Chem. Phys. 125 (2006) 144106–144114.
[62] M.-P. Gaigeot, M. Martinez, R. Vuilleumier, Infrared spectroscopy in the gas and liquid phase from first principle molecular dynamics simulations: application to small peptides, Mol. Phys. 105 (2007) 2857–2878.
[63] L. Gontrani, E. Bodo, A. Triolo, F. Leonelli, P. D'Angelo, V. Migliorati, R. Caminiti, The interpretation of diffraction patterns of two prototypical protic ionic liquids: a challenging task for classical molecular dynamics simulations, J. Phys. Chem. B 116 (2012) 13024–13032.
[64] W. Pohle, D.R. Gauger, H. Fritzsche, B. Rattay, C. Selle, H. Binder, H. Bohlig, FTIR-spectroscopic characterization of phosphocholine-headgroup model compounds, J. Mol. Struct. 563-564 (2001) 463–467.
[65] D. Philip, A. John, C.Y. Panicker, H.T. Varghese, FT-raman, FT-IR and surface enhanced Raman scattering spectra of sodium salicylate, Spectrochim. Acta A 57 (2001) 1561–1566.
[66] B. Humbert, M. Alnot, F. Quiles, Infrared and Raman spectroscopical studies of salicylic and salicylate derivatives in aqueous solution, Spectrochim. Acta A 54 (1998) 465–476.
[67] J.D. Steill, J. Oomens, Action spectroscopy of gas-phase carboxylate anions by multiple photon ir electron detachment/attachment, J Phys. Chem. A 113 (2009) 4941–4946.
[68] J. Oomens, J.D. Steill, Free carboxylate stretching modes, J Phys. Chem. A 112 (2008) 3281–3283.
[69] E. Spinner, The vibration spectra of some substituted acetate ions, J. Chem. Soc. 4217–4226 (1964).
[70] E. Spinner, Vibration-spectral studies of carboxylate ions. Part II. Substituted benzoate ions, J. Chem. Soc B. (1967) 874–879.
[71] S.E. Cabaniss, I.F. McVey, Aqueous infrared carboxylate absorbances: aliphatic monocarboxylates, Spectrochim. Acta A 51 (1995) 2385–2395.